

Energy Preservation and Stability of Random Filterbanks

Daniel Haider, Vincent Lostanlen, Martin Ehler, and Peter Balazs

Abstract—What makes waveform-based deep learning so hard? Despite numerous attempts at training convolutional neural networks (convnets) for filterbank design, they often fail to outperform hand-crafted baselines. This is all the more surprising because these baselines are linear time-invariant systems: as such, their transfer functions could be accurately represented by a convnet with a large receptive field. In this article, we elaborate on the statistical properties of simple convnets from the mathematical perspective of random convolutional operators. We find that FIR filterbanks with random Gaussian weights are ill-conditioned for large filters and locally periodic input signals, which both are typical in audio signal processing applications. Furthermore, we observe that expected energy preservation of a random filterbank is not sufficient for numerical stability and derive theoretical bounds for its expected frame bounds.

Index Terms—Convolutional neural networks, digital filters, audio processing, statistical learning, stability, frame theory.

I. INTRODUCTION

FILTERBANKS are linear time-invariant systems which decompose a signal \mathbf{x} into $J > 1$ subbands. By convolution with filters $(\mathbf{w}_n)_{n=1,\dots,J}$ this yields a multivariate time series $\Phi\mathbf{x}[n, j] = (\mathbf{x} * \mathbf{w}_n)[j]$. Filterbanks play a key role in speech and music processing: constant-Q-transforms, third-octave spectrograms, and Gammatone filterbanks are some well-known examples [1]–[3]. Beyond the important case of audio, filterbanks also serve in other domains such as seismology [4], astrophysics [5], and neuroscience [6].

Over the past decade, the surge of deep learning has made use of filterbank analysis as a prior step to signal classification and generation. In this context, filterbank design is a form of feature engineering. More recently, it has been proposed to replace feature engineering with feature learning: i.e., to optimize filterbank parameters jointly with the rest of the deep learning pipeline [7].

Yet, prior work on filterbank learning has led to mixed results so far. For example, on the TIMIT dataset, using a 1-D convolutional network (convnet) on the “raw waveform” was found to fare poorly (29.2% phone error rate or PER) compared to the mel-spectrogram baseline (17.8% PER) [8]. Interestingly, fixing the convnet weights to form a filterbank on the mel-scale brings the PER to 18.3%, and fine-tuning them by gradient descent, to 17.8%. Similar findings were reported with Gammatone filterbanks [9].

Arguably, such a careful initialization procedure defeats the purpose of deep learning; i.e., sparing the human effort of feature engineering. Furthermore, it contrasts with other

domains (e.g., image processing) in which all convnet layers may simply be initialized as random finite impulse responses (FIR). To our knowledge, the difficulties of learning filterbanks from randomly initialized FIR filters have not yet received a formal justification. Rather, current arguments against FIR filters are based on a qualitative description:

To understand the gap in performance in [8] and [9], we must distinguish neural network architecture design vs. iterative optimization. Simply put: just because a convnet *can* represent a human-engineered filterbank does not mean it *will*. This issue is not just of purely theoretical interest: in some emerging topics of machine listening such as bioacoustics, it would be practically useful to train a randomly initialized FIR filterbank; i.e., with minimal domain-specific knowledge about the acoustic events of interest [10], [11].

The aim of this article is a better understanding of the fundamental mathematical properties of convnets with Gaussian random initialization to explain where the difficulties for deep learning in the raw waveform lie. For this purpose, we treat the decomposition of a finite-length sequence \mathbf{x} by a FIR filterbank via the application of a random convolutional operator Φ . These operators may be interpreted as the first layer of an untrained convnet. We are particularly interested in their energy preservation property, i.e. how $\|\Phi\mathbf{x}\|^2$ and $\|\mathbf{x}\|^2$ relate. This naturally leads further to the discussion on the numerical stability of Φ , which is a crucial prerequisite for stable dynamics in gradient-based optimization [12]. While there are several approaches investigating filterbanks applied to random signals, in particular noisy signals, a discussion of filterbanks with random entries is missing.

In Section II we set up the mathematical paradigm for random filterbanks Φ and provide formulas for the expected value and variance of the squared Euclidean norm $\|\Phi\mathbf{x}\|^2$ for known input \mathbf{x} . Section III computes bounds for the expected values of the frame bounds of the filterbank as a generalized shift-invariant system, i.e. lower and upper bounds of $\|\Phi\mathbf{x}\|^2$ for any unit norm \mathbf{x} and draws the link to energy preservation properties of Φ .

II. FIR FILTERBANK WITH RANDOM GAUSSIAN WEIGHTS

Throughout this article, we use finite circulant convolution. To provide an algebraic setting for it, we consider the indices of any signal \mathbf{x} and any filter \mathbf{w} within the ring $\mathbb{Z}_N = \mathbb{Z} \bmod N$, i.e. $\mathbf{x}[n + kN] = \mathbf{x}[n]$ for any $k \in \mathbb{N}$. Furthermore, we assume the filters to have support length $T \leq N$, implicitly padded with $N - T$ zeros at the end. Then, the circular convolution of a signal \mathbf{x} with a filter \mathbf{w} is given as $(\mathbf{x} * \mathbf{w})[n] = \sum_{k=0}^{N-1} \mathbf{x}[k] \mathbf{w}[(n - k) \bmod N]$. We shall write $\mathbf{x}, \mathbf{w} \in \mathbb{R}^N$ and refer to T as the length

D. Haider and P. Balazs are with the Acoustics Research Institute, Austrian Academy of Sciences, Vienna, Austria. V. Lostanlen is with Nantes Université, École Centrale Nantes, CNRS, LS2N, UMR 6004, F-44000 Nantes, France. M. Ehler is with University of Vienna, Faculty of Mathematics, Vienna, Austria.

of the filter. Finally, we use the norms $\|\mathbf{x}\|_2 = (\sum_{k=0}^{N-1} |x[k]|^2)^{\frac{1}{2}}$ and $\|\mathbf{x}\|_\infty = \max_{k=0,\dots,N-1} |x[k]|$.

A. Moments of the squared Euclidean norm

Our first result reveals the moments of the squared Euclidean norm – or energy – of the filter bank coefficients. For this, recall the circular auto-correlation of a signal $\mathbf{x} \in \mathbb{R}^N$,

$$\mathbf{R}_{\mathbf{x}\mathbf{x}}(t) = \sum_{k=0}^{N-1} \mathbf{x}[k] \mathbf{x}[(k-t) \bmod N].$$

Proposition II.1. *Let $\mathbf{x} \in \mathbb{R}^N$ and Φ a random filterbank with J i.i.d. filters $\mathbf{w}_j \sim \mathcal{N}(0, \sigma^2 \mathbf{I})$ of length $T \leq N$. The squared Euclidean norm of $\Phi \mathbf{x}$ has an expected value of*

$$\mathbb{E}[\|\Phi \mathbf{x}\|^2] = JT \sigma^2 \|\mathbf{x}\|^2 \quad (1)$$

and a variance of

$$\mathbb{V}[\|\Phi \mathbf{x}\|^2] = 2J \sigma^4 \sum_{\tau=-T}^T (T - |\tau|) \mathbf{R}_{\mathbf{x}\mathbf{x}}(\tau)^2. \quad (2)$$

Hence, when the filterbank is scaled via $\sigma^2 = (JT)^{-1}$, one can expect energy preservation. Note that JT is the number of parameters in the filterbank. However, the larger the auto-correlation of the signal is, the larger the variance becomes. Our proof of Proposition II.1 hinges on the following lemmata, which are themselves proven in the appendix. The main idea is to introduce the circulant shifts to the deterministic signal \mathbf{x} , instead of to the random filters \mathbf{w}_j , as it is usually done for generalized shift-invariant systems.

Lemma II.2. *Let $\mathbf{x}, \mathbf{w} \in \mathbb{R}^N$ with \mathbf{w} of length $T \leq N$. The circular convolution of \mathbf{x} and \mathbf{w} satisfies $\|\mathbf{x} * \mathbf{w}\|^2 = \mathbf{w}^\top \mathbf{Q}_T(\mathbf{x}) \mathbf{w}$, where the entries of the matrix $\mathbf{Q}_T(\mathbf{x})$ are given by $\mathbf{Q}_T(\mathbf{x})[n, t] = \mathbf{R}_{\mathbf{x}\mathbf{x}}((n-t) \bmod N)$ for each $0 \leq n, t < T-1$.*

Lemma II.3. *Let $\mathbf{x} \in \mathbb{R}^N$. All diagonal entries of the matrix $\mathbf{Q}_T(\mathbf{x})$ from Lemma II.2 are equal to $\|\mathbf{x}\|^2$.*

Proof of Proposition II.1. Given a filter \mathbf{w}_j for $1 \leq j \leq J$, we apply Lemma II.2 and use the cyclic property of the trace:

$$\|\mathbf{x} * \mathbf{w}_j\|^2 = \text{Tr}(\mathbf{w}_j^\top \mathbf{Q}_T(\mathbf{x}) \mathbf{w}_j) = \text{Tr}(\mathbf{Q}_T(\mathbf{x}) \mathbf{w}_j \mathbf{w}_j^\top). \quad (3)$$

We take the expected value on both sides and recognize the term $\mathbb{E}[\mathbf{w}_j \mathbf{w}_j^\top]$ as the covariance matrix of \mathbf{w}_j , i.e., $\sigma^2 \mathbf{I}$:

$$\mathbb{E}[\|\mathbf{x} * \mathbf{w}_j\|^2] = \text{Tr}(\mathbf{Q}_T(\mathbf{x}) \mathbb{E}[\mathbf{w}_j \mathbf{w}_j^\top]) = \sigma^2 \text{Tr}(\mathbf{Q}_T(\mathbf{x})). \quad (4)$$

By Lemma II.3, $\text{Tr}(\mathbf{Q}_T(\mathbf{x})) = T \|\mathbf{x}\|^2$, hence $\mathbb{E}[\|\mathbf{x} * \mathbf{w}_j\|^2] = \sigma^2 T \|\mathbf{x}\|^2$. For the variance, we recall Theorem 5.2 from [13], which states that if $\mathbf{v} \sim \mathcal{N}(\boldsymbol{\mu}, \boldsymbol{\Sigma})$, then for any matrix \mathbf{A} :

$$\mathbb{V}[\mathbf{v}^\top \mathbf{A} \mathbf{v}] = 2 \text{Tr}(\mathbf{A} \boldsymbol{\Sigma} \mathbf{A} \boldsymbol{\Sigma}) + 4 \boldsymbol{\mu}^\top \mathbf{A} \boldsymbol{\Sigma} \mathbf{A} \boldsymbol{\mu} \quad (5)$$

We set $\mathbf{v} = \mathbf{w}_j$, $\boldsymbol{\mu} = \mathbf{0}$, $\boldsymbol{\Sigma} = \sigma^2 \mathbf{I}$, and $\mathbf{A} = \mathbf{Q}_T(\mathbf{x})$ and obtain:

$$\begin{aligned} \mathbb{V}[\|\mathbf{x} * \mathbf{w}_j\|^2] &= 2 \sigma^4 \text{Tr}(\mathbf{Q}_T(\mathbf{x})^2) \\ &= 2 \sigma^4 \sum_{t=0}^{T-1} \sum_{t'=0}^{T-1} \mathbf{R}_{\mathbf{x}\mathbf{x}}(t-t') \mathbf{R}_{\mathbf{x}\mathbf{x}}(t'-t) \\ &= 2 \sigma^4 \sum_{t=0}^{T-1} \sum_{\tau=-t}^{T-1-t} \mathbf{R}_{\mathbf{x}\mathbf{x}}(\tau)^2. \end{aligned} \quad (6)$$

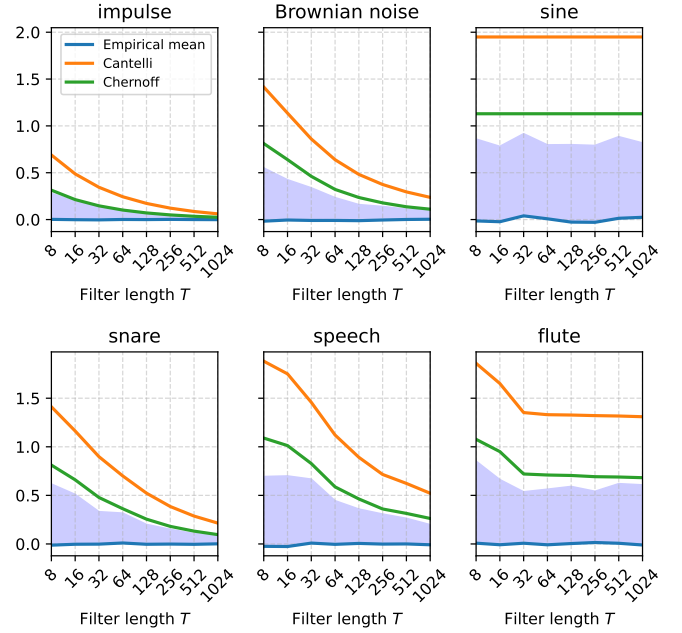


Fig. 1. The blue curve shows empirical means and 0.95-quantiles of 500 realizations of $\|\Phi \mathbf{x}\|^2 - \|\mathbf{x}\|^2$ for different signals \mathbf{x} with $\|\mathbf{x}\| = 1$. The filter lengths are $T = 2^k$ for $k = 3, 4, \dots, 10$ and $J = 10$. The orange curves show the values of α in Proposition II.4 such that the RHS of (7) equals 0.05 and the green curves show the values of α such that the RHS of (8) equals 0.05 for every T , such that we obtain bounds for the 0.95-quantiles by means of the derived bounds.

By a simple combinatorial argument, the sums above can be written as $\sum_{\tau=-T}^T (T - |\tau|) \mathbf{R}_{\mathbf{x}\mathbf{x}}(\tau)^2$. The proof concludes by the independence of the J filters in Φ . ■

Using the results of Proposition II.1 we can derive two estimations for the probability of relative energy deviation of the filterbank coefficients. The proofs can be found in the appendix.

Proposition II.4. *Let Φ be a random filterbank with J i.i.d. filters $\mathbf{w}_j \sim \mathcal{N}(0, \sigma^2 \mathbf{I})$ of length T and $\sigma^2 = (JT)^{-1}$. Given a finite real sequence $\mathbf{x} \neq \mathbf{0}$ and let $\boldsymbol{\lambda} = (\lambda_k)_{k=0,\dots,T-1}$ denote the vector of eigenvalues of $\mathbf{Q}_T(\mathbf{x})$, the probability of relative deviation between $\|\Phi \mathbf{x}\|^2$ and $\|\mathbf{x}\|^2$ is bounded from above as:*

$$\mathbb{P}\left[\frac{\|\Phi \mathbf{x}\|^2 - \|\mathbf{x}\|^2}{\|\mathbf{x}\|^2} \geq \alpha\right] \leq \frac{\mathbb{V}[\|\Phi \mathbf{x}\|^2]}{\mathbb{V}[\|\Phi \mathbf{x}\|^2] + \alpha^2 \mathbf{R}_{\mathbf{x}\mathbf{x}}(0)^2} \quad (7)$$

and

$$\mathbb{P}\left[\frac{\|\Phi \mathbf{x}\|^2 - \|\mathbf{x}\|^2}{\|\mathbf{x}\|^2} \geq \alpha\right] \leq \exp\left(-\frac{\alpha^2 JT^2 \|\mathbf{x}\|^4}{2\alpha T \|\boldsymbol{\lambda}\|_\infty \|\mathbf{x}\|^2 + 2\|\boldsymbol{\lambda}\|_2^2}\right). \quad (8)$$

Both bounds have their different merits. The upper bound in Inequality (7), based on Cantelli's (or one-sided Chebyshev's) inequality [14], is very basic as it only makes use of the variance but well-interpretable via the auto-correlation of the input signal. The higher the auto-correlation is, the higher the variance of $\|\Phi \mathbf{x}\|^2$ becomes according to (2), hence, the worse the bound becomes. Since audio signals are naturally locally periodic and, hence, have high auto-correlation, random filterbanks applied to such signals suffer from instabilities

particularly.

The bound in Inequality (8), based on Chernoff's inequality [15], is much tighter by using the moment generating function and relates to the eigenvalues of the matrix $\mathbf{Q}_T(\mathbf{x})$. For $T < N$, $\mathbf{Q}_T(\mathbf{x})$ is a symmetric Toeplitz matrix, whose eigenvalues are not known explicitly in general. This makes the interpretation in terms of properties of \mathbf{x} more difficult. For $T = N$, $\mathbf{Q}_T(\mathbf{x})$ is additionally circulant, hence, the eigenvalues coincide with the squared modulus of the DFT of the input signal, i.e. $\lambda = |\hat{x}|^2$.

B. Numerical simulation

Due to the dependence of the variance of $\|\Phi\mathbf{x}\|^2$ on the auto-correlation of \mathbf{x} we expect the signal class of \mathbf{x} to be a relevant aspect for the stability of Φ . We elaborate on this thought by considering three artificial signals from different signal classes: (i) a single impulse, which has low auto-correlation, (ii) a Brownian noise signal modeled by a random walk which has medium auto-correlation and (iii) a sine wave with frequency $\omega = \pi$, which has high auto-correlation. For each of these signals, we compute the empirical mean of 500 realizations of $\|\Phi\mathbf{x}\|^2$ for increasing filter length, see Figure 1. The experiment reflects well that for signals with low auto-correlation, the variance of energy of the filterbank coefficients decreases as the filters become larger. For highly auto-correlated signals, this benefit ceases. Note that J is chosen such that $J \geq \log(T)$. This behavior perfectly transfers to real-world signals with respective characteristics: a snare drum, a speech, and a flute signal. Spectrograms of these signals are provided in the appendix.

III. EXTREME VALUE THEORY MEETS FRAME THEORY

We now analyze $\|\Phi\mathbf{x}\|^2$ via the properties of Φ as a linear operator, i.e. independent of \mathbf{x} . In notions of frame theory, Φ plays the role of the analysis operator associated with the generalized shift-invariant system comprising all filters of Φ and its (circulant) translates. If there are numbers $0 < A \leq B$ such that

$$A\|\mathbf{x}\|^2 \leq \|\Phi\mathbf{x}\|^2 \leq B\|\mathbf{x}\|^2 \quad (9)$$

holds for any $\mathbf{x} \in \mathbb{R}^N$, we say the filterbank forms a *frame* for \mathbb{R}^N with lower and upper frame bounds A, B respectively. The optimal frame bounds can be computed as:

$$A = \min_{\|\mathbf{x}\|_2=1} \|\Phi\mathbf{x}\|^2, \quad B = \max_{\|\mathbf{x}\|_2=1} \|\Phi\mathbf{x}\|^2. \quad (10)$$

For fixed Φ , the ratio $\kappa = \frac{B}{A}$ yields its condition number, determining the numerical stability of the linear transform associated with Φ . Moreover, $\kappa = 1$ if and only if Φ preserves energy up to a scaling factor $C > 0$, i.e. $\|\Phi\mathbf{x}\|^2 = C\|\mathbf{x}\|^2$. This seems to not hold for the expected values of κ and $\|\Phi\mathbf{x}\|^2$ and heavily depend on the number of filters J and their length T , see Figure 2. In this sense, choosing $\sigma^2 = (TJ)^{-1}$ indeed provides expected energy preservation of a random filterbank by Equation (1) but does not guarantee it to be well-conditioned in expectation. Since A and B are dependent random variables, $\mathbb{E}[\kappa]$ is difficult to study analytically [16]. In this article, we focus on the expected values of A and B separately. Yet, it is unclear how $\mathbb{E}[\kappa]$ and $\frac{\mathbb{E}[B]}{\mathbb{E}[A]}$ relate. The top plot in Figure 2 compares empirical computations of the expectations of

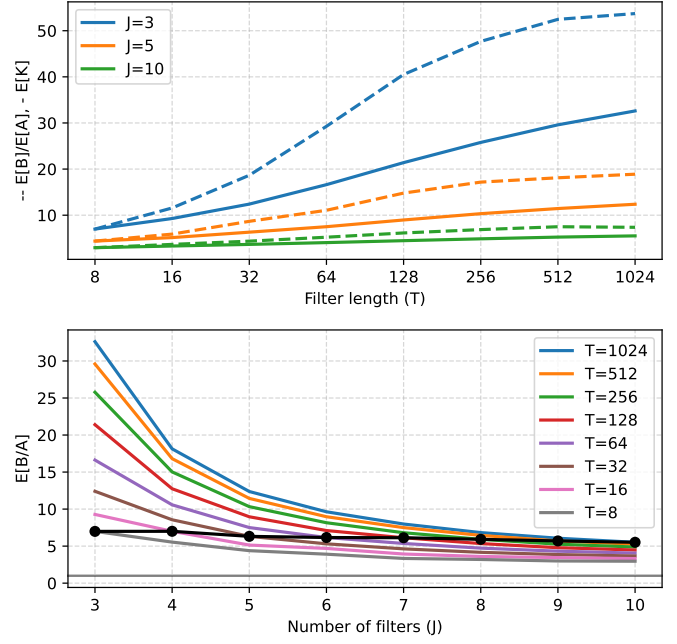


Fig. 2. Top: Empirical computations of $\mathbb{E}[\kappa]$ (solid) and $\mathbb{E}[B]/\mathbb{E}[A]$ (dashed) over 200 iterations are plotted against increasing filter lengths T for different numbers of filters J . Bottom: Empirical computations of $\mathbb{E}[\kappa]$ are plotted against increasing numbers of filters J for different values of filter lengths T . For the scaling law $J = \log(T)$ (solid black), κ stays approximately constant.

both quantities for increasing filter lengths T and different numbers of filters J . For all tested settings we obtain $\mathbb{E}[\kappa] \leq \frac{\mathbb{E}[B]}{\mathbb{E}[A]}$, suggesting an upper bound. The bottom plot in Figure 2 shows empirical computations of $\mathbb{E}[\kappa]$ for increasing number of filters J for different filter lengths T . The solid black line indicates $J = \log(T)$. We come back to this in Section III-B.

A. From quadratic forms to chi-squared distributions

Although the expected frame bounds $\mathbb{E}[A]$ and $\mathbb{E}[B]$ do not have closed-form expressions, we can relate them to the expected order statistics of the chi-squared distribution with J degrees of freedom, denoted by $\chi^2(J)$.

Theorem III.1. *Let Φ be a random filterbank with J i.i.d. filters $\mathbf{w}_j \sim \mathcal{N}(0, \sigma^2 \mathbf{I})$ with $\sigma^2 = (JT)^{-1}$. The optimal frame bounds A, B of Φ satisfy $\mathbb{E}[A] \leq 1 \leq \mathbb{E}[B]$ and are bounded in expectation by the order statistics of $Y_0, \dots, Y_{T-1} \sim \chi^2(J)$ i.i.d. chi-squared distributed with J degrees of freedom:*

$$\mathbb{E}[A] \geq J^{-1} \mathbb{E} \left[\min_{0 \leq k \leq T-1} Y_k \right], \quad (11)$$

$$\mathbb{E}[B] \leq J^{-1} \mathbb{E} \left[\max_{0 \leq k \leq T-1} Y_k \right]. \quad (12)$$

Proof. Clearly, $\mathbb{E}[\|\Phi\mathbf{x}\|^2] = C\|\mathbf{x}\|^2$ immediately implies $\mathbb{E}[A] \leq C \leq \mathbb{E}[B]$. By Proposition II.1 and $\sigma^2 = (JT)^{-1}$, $C = 1$. For the second part, we consider the eigenvalue decomposition of $\mathbf{Q}_T(\mathbf{x}) = \mathbf{U}\mathbf{\Lambda}\mathbf{U}^*$. The columns of \mathbf{U} are the eigenvectors of $\mathbf{Q}_T(\mathbf{x})$ and $\mathbf{\Lambda}$ has the eigenvalues λ_k on its main diagonal. It is crucial to notice that \mathbf{U} is an orthogonal matrix since $\mathbf{Q}_T(\mathbf{x})$

is symmetric. For any filter \mathbf{w}_j , $1 \leq j \leq J$ let $\mathbf{y}_{j,k}$ denote the k -th component of the random vector $\mathbf{y}_j = U^\top \mathbf{w}_j$. By Lemma II.2 we obtain:

$$\|\mathbf{x} * \mathbf{w}_j\|^2 = \mathbf{w}_j^\top U^\top \Lambda U \mathbf{w}_j = \sum_{k=0}^{T-1} \lambda_k \mathbf{y}_{j,k}^2. \quad (13)$$

Let $Y_k = \sum_{j=1}^J \frac{\mathbf{y}_{j,k}^2}{\sigma^2}$, then using (13) yields:

$$\|\Phi \mathbf{x}\|^2 = \sum_{j=1}^J \|\mathbf{x} * \mathbf{w}_j\|^2 = \sigma^2 \sum_{k=0}^{T-1} \lambda_k \sum_{j=1}^J \frac{\mathbf{y}_{j,k}^2}{\sigma^2} = \sigma^2 \sum_{k=0}^{T-1} \lambda_k Y_k. \quad (14)$$

By orthogonality of U , \mathbf{y}_j follows the same distribution as \mathbf{w}_j . This can be seen by $U^\top \mathbf{w}_j \sim \mathcal{N}(0, \sigma^2 U \mathbf{I} U^\top) = \mathcal{N}(0, \sigma^2 \mathbf{I})$.

Since $\frac{\mathbf{y}_{j,k}^2}{\sigma^2}$ are i.i.d. standard Gaussian random variables, we find Y_k to be i.i.d. chi-squared distributed with J degrees of freedom for every $k = 0, \dots, T-1$, i.e. $Y_k \sim \chi^2(J)$. Using the associated order statistics

$$Y_T^{\min} = \min_{0 \leq k \leq T-1} Y_k \quad \text{and} \quad Y_T^{\max} = \max_{0 \leq k \leq T-1} Y_k \quad (15)$$

as lower, respectively upper bound for Y_k in (14) and that $\sum_{k=0}^{T-1} \lambda_k = \text{Tr}(\mathbf{Q}_T(\mathbf{x})) = T \|\mathbf{x}\|^2$ (see Lemma II.3), we obtain:

$$A = \min_{\|\mathbf{x}\|_2=1} \|\Phi \mathbf{x}\|^2 \geq \sigma^2 T Y_T^{\min},$$

$$B = \max_{\|\mathbf{x}\|_2=1} \|\Phi \mathbf{x}\|^2 \leq \sigma^2 T Y_T^{\max}.$$

Taking the expectation on both sides and setting $\sigma^2 = (JT)^{-1}$ yields the claim. ■

Hence, a random filterbank is a frame almost surely, however, numerical instabilities are induced for large filters. Figure 3 shows empirical computations of Inequalities (11) and (12). The plot reflects the theoretical derivations well.

Unfortunately, the order statistics of the chi-squared distribution are generally not available in closed form [17]. Via asymptotic assumptions, we shall obtain a clearer picture.

B. Asymptotic Behavior

For large J a chi-squared distribution with J degrees of freedom resembles a Gaussian distribution with mean J and variance $2J$ [18]. In such a scenario, we shall assume the Y_k in Theorem III.1 to be distributed accordingly.

Proposition III.2. *Let Φ be a random filterbank with J i.i.d. filters of length $T \leq N$. Let A, B denote the optimal frame bounds of Φ and assume $Y_k = \tilde{Y}_k \sim \mathcal{N}(J, 2J)$ for the Y_k in Theorem III.1. For large T we have*

$$\mathbb{E}[A] \geq 1 - 2\sqrt{\frac{\log(T)}{J}} \quad \text{and} \quad \mathbb{E}[B] \leq 1 + 2\sqrt{\frac{\log(T)}{J}}. \quad (16)$$

Taming $\mathbb{E}[B]$ for $T \rightarrow \infty$ in terms of the above bound requires to choose $J \geq \log(T)$. For equality, this corresponds to a classic scaling law often used in signal processing, e.g. for the design of wavelet bases [19]. Respecting this scaling law in our setting provides approximately constant numerical condition numbers $\mathbb{E}[\kappa]$, illustrated in Figure 2. Interestingly, we do not observe this behavior for $\frac{\mathbb{E}[B]}{\mathbb{E}[A]}$. The upper bound for $\mathbb{E}[B]$ in (16) is

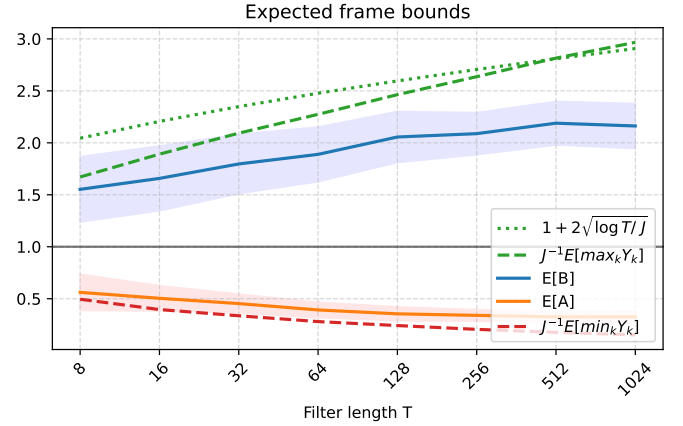


Fig. 3. The plot shows the divergence of empirical means of 500 upper and lower frame bounds of random filterbanks with $\sigma^2 = (JT)^{-1}$. The filters are chosen to have lengths of $T = 2^l$ for $l = 3, 4, \dots, 10$. The number of filters $J = 10$ is chosen to fulfill $J \geq \log(T)$. The dashed lines indicate experimental computations of the bounds derived in Inequalities (11) (red) and (12) (green) and the dotted line represents the upper bound of $\mathbb{E}[B]$ from Inequality (16).

plotted as dotted line in Figure 3.

In order to have $\mathbb{E}[A] > 0$ in terms of the bound in (16) it is required to choose $J > 4 \log(T)$. This, however, does not reflect the practice well and other approximations are desirable.

IV. CONCLUSION

In the presented article, we introduce a mathematical perspective of filterbanks with randomly initialized filters via random convolutional operators. We derive basic statistical properties of the energy of such filterbanks applied to a signal and find a low auto-correlation of the signal to be the key property for expecting energy preservation with little variance. In this sense, highly auto-correlated signals, such as periodic signals are adversarial examples of potential instabilities. Furthermore, by viewing filterbanks as generalized shift-invariant systems, we show that expected energy preservation is not sufficient for numerical stability and heavily depends on the choice of the number of filters J and their length T . Via theoretical bounds for the frame bounds of a filterbank by means of the chi-squared distribution and asymptotic assumptions we encounter the classical scaling law $J = \log(T)$. A theoretical analysis of the expected condition number remains an open problem.

ACKNOWLEDGMENT

D. Haider is recipient of a DOC Fellowship of the Austrian Academy of Sciences at the Acoustics Research Institute (A 26355). V. Lostanlen is supported by ANR MuReNN. The work of M. Ehler was supported by the WWTF project CHARMED (VRG12-009) and P. Balazs was supported by the FWF projects LoFT (P 34624) and NoMASP (P 34922).

REFERENCES

- [1] T. Necciari, N. Holighaus, P. Balazs, Z. Průša, P. Majdak, and O. Derrien, "Audlet filter banks: A versatile analysis/synthesis framework using auditory frequency scales," *Applied Sciences*, vol. 8, no. 1, 2018. [Online]. Available: <https://www.mdpi.com/2076-3417/8/1/96>
- [2] P. Balazs, N. Holighaus, T. Necciari, and D. Stoeva, *Frame Theory for Signal Processing in Psychoacoustics*. Cham: Springer International Publishing, 2017, pp. 225–268. [Online]. Available: https://doi.org/10.1007/978-3-319-54711-4_10
- [3] R. F. Lyon, *Human and machine hearing: Extracting meaning from sound*. Cambridge University Press, 2017.
- [4] M.-A. Meier, T. Heaton, and J. Clinton, "The Gutenberg algorithm: Evolutionary Bayesian magnitude estimates for earthquake early warning with a filter bank," *Bulletin of the Seismological Society of America*, vol. 105, no. 5, pp. 2774–2786, 2015.
- [5] E. Chassande-Mottin, "Learning approach to the detection of gravitational wave transients," *Physical Review D*, vol. 67, no. 10, p. 102001, 2003.
- [6] K. K. Ang, Z. Y. Chin, H. Zhang, and C. Guan, "Filter bank common spatial pattern (FBCSP) in brain-computer interface," in *Proc. IEEE IJCNN*. IEEE, 2008, pp. 2390–2397.
- [7] M. Dörfler, T. Grill, R. Bammer, and A. Flexer, "Basic filters for convolutional neural networks applied to music: Training or design?" *Neural Computing and Applications*, vol. 32, pp. 941–954, 2020.
- [8] N. Zeghidour, N. Usunier, I. Kokkinos, T. Schaiz, G. Synnaeve, and E. Dupoux, "Learning filterbanks from raw speech for phone recognition," in *Proc. IEEE ICASSP*. IEEE, 2018, pp. 5509–5513.
- [9] T. Sainath, R. J. Weiss, K. Wilson, A. W. Senior, and O. Vinyals, "Learning the speech front-end with raw waveform CLDNNs," in *Proc. INTERSPEECH*, 2015.
- [10] S. L. Hopp, M. J. Owren, and C. S. Evans, *Animal acoustic communication: sound analysis and research methods*. Springer Science & Business Media, 2012.
- [11] D. Stowell, "Computational bioacoustics with deep learning: A review and roadmap," *PeerJ*, vol. 10, p. e13152, 2022.
- [12] I. J. Goodfellow, Y. Bengio, and A. Courville, *Deep Learning*. Cambridge, MA, USA: MIT Press, 2016, <http://www.deeplearningbook.org>.
- [13] A. C. Rencher and G. B. Schaalje, *Linear models in statistics*. John Wiley & Sons, 2008.
- [14] W. Feller, *An introduction to probability theory and its applications. Vol. I*, ser. Third edition. New York: John Wiley & Sons Inc., 1968.
- [15] H. Chernoff, "A Measure of Asymptotic Efficiency for Tests of a Hypothesis Based on the sum of Observations," *The Annals of Mathematical Statistics*, vol. 23, no. 4, pp. 493 – 507, 1952.
- [16] G. Barrera Vargas and P. Manrique-Mirón, "The asymptotic distribution of the condition number for random circulant matrices," *Extremes*, vol. 25, 2022.
- [17] G. Casella and R. Berger, *Statistical Inference*. Cengage Learning, 2021.
- [18] E. Lehmann and J. Romano, *Testing Statistical Hypotheses*, ser. Springer Texts in Statistics. Springer, 2006.
- [19] S. Mallat, *A Wavelet Tour of Signal Processing: The Sparse Way*, 3rd ed. USA: Academic Press, Inc., 2008.
- [20] L. Birgé and P. Massart, "Minimum contrast estimators on sieves: exponential bounds and rates of convergence," *Bernoulli*, vol. 4, no. 3, pp. 329 – 375, 1998.
- [21] B. Laurent and P. Massart, "Adaptive estimation of a quadratic functional by model selection," *Annals of Statistics*, vol. 28, 10 2000.
- [22] S. Coles, *An Introduction to Statistical Modeling of Extreme Values*, ser. Springer Series in Statistics. Springer London, 2013.

V. APPENDIX

Proof of Lemma II.2. For $\mathbf{x} \in \mathbb{R}^N$ and $\mathbf{w} \in \mathbb{R}^N$ with support at the first $T \leq N$ entries we can write their circulant convolution as left-multiplication of \mathbf{w} by the matrix

$$\mathbf{C}_T(\mathbf{x}) = \begin{pmatrix} \mathbf{x}[0] & \mathbf{x}[1] & \cdots & \mathbf{x}[T-1] \\ \mathbf{x}[N-1] & \mathbf{x}[0] & \cdots & \mathbf{x}[T-2] \\ \vdots & \vdots & & \vdots \\ \mathbf{x}[2] & \mathbf{x}[3] & \cdots & \mathbf{x}[T+1] \\ \mathbf{x}[1] & \mathbf{x}[2] & \cdots & \mathbf{x}[T] \end{pmatrix},$$

i.e. $(\mathbf{x} * \mathbf{w}) = \mathbf{C}_T(\mathbf{x})\mathbf{w}$. The $N \times T$ matrix $\mathbf{C}_T(\mathbf{x})$ is the restriction of the circulant matrix generated by \mathbf{x} to its first T columns and has entries $\mathbf{C}_T(\mathbf{x})[n, t] = \mathbf{x}[(t-n) \bmod N]$ for $n = 0, \dots, N-1$ and $t = 0, \dots, T-1$. By expanding its squared Euclidean norm the quadratic form gets revealed:

$$\begin{aligned} \|\mathbf{x} * \mathbf{w}\|^2 &= \langle \mathbf{C}_T(\mathbf{x})\mathbf{w}, \mathbf{C}_T(\mathbf{x})\mathbf{w} \rangle \\ &= \langle \mathbf{w}, \mathbf{C}_T(\mathbf{x})^\top \mathbf{C}_T(\mathbf{x})\mathbf{w} \rangle \\ &= \mathbf{w}^\top \mathbf{Q}_T(\mathbf{x})\mathbf{w}, \end{aligned}$$

where $\mathbf{Q}_T(\mathbf{x}) = \mathbf{C}_T(\mathbf{x})^\top \mathbf{C}_T(\mathbf{x})$. Recall the circular autocorrelation associated with \mathbf{x} to be given as $\mathbf{R}_{\mathbf{xx}}(t) = \sum_{k=0}^{N-1} \mathbf{x}[k]\mathbf{x}[(k-t) \bmod N]$. A straightforward computation reveals the entries of $\mathbf{Q}_T(\mathbf{x})$ to be given in terms of $\mathbf{R}_{\mathbf{xx}}$:

$$\begin{aligned} \mathbf{Q}_T(\mathbf{x})[n, t] &= \sum_{k=0}^{N-1} \mathbf{x}[(n-k) \bmod N] \mathbf{x}[(t-k) \bmod N] \\ &= \mathbf{R}_{\mathbf{xx}}((n-t) \bmod N). \end{aligned}$$

Proof of Lemma II.3. For every $t = 0, \dots, T-1$:

$$\mathbf{Q}_T(\mathbf{x})[t, t] = \mathbf{R}_{\mathbf{xx}}(0) = \sum_{k=0}^{N-1} \mathbf{x}[k]^2 = \|\mathbf{x}\|^2 \quad (17)$$

by application of Lemma II.2. ■

In order to proof Proposition II.4 we use the following lemma. A proof can be found in the proof of Lemma 8 in [20].

Lemma V.1 (Adapted from Birgé et al. (1998)). *For any $v, c, \beta > 0$,*

$$\inf_{\mu > 0} \frac{\mu^2 v^2}{1 - 2\mu c} - \mu\beta \leq -\frac{\beta^2}{2c\beta + 2v^2}.$$

Proof of Proposition II.4. Let $\beta > 0$ and $\mathbf{x} \in \mathbb{R}^N$. We show (7) via Cantelli's inequality for any random variable Z with finite mean and variance [14]:

$$\mathbb{P}[Z - \mathbb{E}[Z] \geq \beta] \leq \frac{\mathbb{V}[Z]}{\mathbb{V}[Z] + \beta^2}. \quad (18)$$

We set $Z = \|\Phi\mathbf{x}\|^2$, $\beta = \alpha\|\mathbf{x}\|^2$ and apply Proposition II.1. Replacing $\|\mathbf{x}\|^4$ by $\mathbf{R}_{\mathbf{xx}}[0]^2$ and $J\sigma^4$ by $J^{-1}T^{-2}$ shows the claim.

We show (8) via the generic Chernoff bounds for any random variable Z :

$$\mathbb{P}[Z \geq \beta] \leq \inf_{\mu > 0} \mathbb{E}[e^{\mu Z}] e^{-\mu\beta}. \quad (19)$$

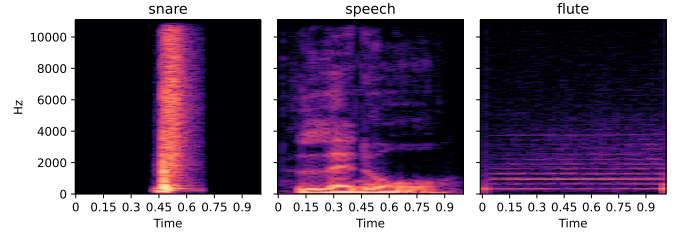


Fig. 4. Via the spectrograms of the real-world signals described in Section II-B one can get a visual impression of their different auto-correlations: The snare has low, the speech signal medium and the flute high auto-correlation.

We set $Z = \|\Phi\mathbf{x}\|^2 - \|\mathbf{x}\|^2$ and use (14) together with a straightforward computation to see that

$$\log \mathbb{E}[e^{\mu Z}] = \sum_{k=0}^{T-1} \sum_{j=1}^J \log \mathbb{E}[\exp(\mu \sigma^2 \lambda_k (y_{j,k}^2 - 1))].$$

Recall that $\frac{y_{j,k}}{\sigma^2} \sim \mathcal{N}(0, 1)$. Analog to the proof of Lemma 1 in [21], we use that the mapping $\psi : u \mapsto \log \mathbb{E}[\exp(u \sigma^2 (X^2 - 1))]$ satisfies $\psi(u) \leq \frac{u^2 \sigma^4}{1 - 2u \sigma^2}$ for any $X \sim \mathcal{N}(0, 1)$ and $0 < u < \frac{1}{2\sigma^2}$. Since $\mathbf{C}_T(\mathbf{x})$ is a principal submatrix of a positive definite matrix (autocorrelation matrix), $\lambda_k > 0$ for all $k = 0, \dots, T-1$. Therefore, for $\mu < \frac{1}{2\sigma^2 \max_k \lambda_k}$,

$$\log \mathbb{E}[e^{\mu Z}] \leq \sum_{k=0}^{T-1} \sum_{j=1}^J \frac{(\mu \lambda_k)^2 \sigma^4}{1 - 2\mu \sigma^2 \lambda_k} \leq \frac{\mu^2 \sigma^4 J \|\boldsymbol{\lambda}\|_2^2}{1 - 2\mu \sigma^2 \|\boldsymbol{\lambda}\|_\infty}. \quad (20)$$

Finally, using (20) and Lemma V.1 with $v^2 = \sigma^4 J \|\boldsymbol{\lambda}\|_2^2$ and $c = \sigma^2 \|\boldsymbol{\lambda}\|_\infty$, we obtain

$$\begin{aligned} \inf_{\mu > 0} \mathbb{E}[e^{\mu Z}] e^{-\mu\beta} &= \exp\left(\inf_{\mu > 0} \log \mathbb{E}[e^{\mu Z}] - \mu\beta\right) \\ &\leq \exp\left(\inf_{\mu > 0} \frac{\mu^2 \sigma^4 J \|\boldsymbol{\lambda}\|_2^2}{1 - 2\mu \sigma^2 \|\boldsymbol{\lambda}\|_\infty} - \mu\beta\right) \\ &\leq \exp\left(-\frac{\beta^2}{2\beta \sigma^2 \|\boldsymbol{\lambda}\|_\infty + 2\sigma^4 J \|\boldsymbol{\lambda}\|_2^2}\right). \end{aligned}$$

Setting $\beta = \alpha\|\mathbf{x}\|^2$ and $\sigma^2 = (JT)^{-1}$ yields the claim. ■

Proof of Proposition III.2. We make use of the fact that the maximum of T normal i.i.d. random variables can be asymptotically approximated by $\sqrt{2\log(T)}$ and the minimum by $-\sqrt{2\log(T)}$, see e.g. [22]. Hence, for $\tilde{Y}_k \sim J + \sqrt{2J}\mathcal{N}(0, 1)$, we obtain for $\tilde{Y}_T^{\max} = \max_{0 \leq k \leq T-1} \tilde{Y}_k$ that

$$\mathbb{E}[\tilde{Y}_T^{\max}] \rightarrow J + \sqrt{2J}\sqrt{2\log(T)} = J + 2\sqrt{J\log(T)}$$

as $T \rightarrow \infty$. An analogous equation holds for $\tilde{Y}_T^{\min} = \min_{0 \leq k \leq T-1} \tilde{Y}_k$. Multiplying by J^{-1} yields the result. ■

Remark. One can derive the relation

$$\mathbb{E}[\kappa] = \frac{\mathbb{E}[B]}{\mathbb{E}[A]} - \frac{\text{Cov}[A, \kappa]}{\mathbb{E}[A]},$$

where the upper plot in Figure 2 suggests that $\text{Cov}[A, \kappa] > 0$. If and under which conditions this is indeed true is left as an open question.

The code for reproducing all experiments can be found under <https://github.com/danedane-haider/Random-Filterbanks>.